Syngas Production Using a Catalytic Engine

by

Andrea Arce

Submitted to the
Department of Mechanical Engineering
in Partial Fulfillment of the Requirements for the Degree of

Bachelor of Science in Mechanical Engineering

at the

Massachusetts Institute of Technology

June 2015

Signature redacted

Signature of Author: _____
Department of Mechanical Engineering
May 8, 2015

Signature redacted

Certified by: _____
John G. Brisson
Professor of Mechanical Engineering
Thesis Supervisor

Signature redacted

Accepted by: _____
Anette Hosoi
Professor of Mechanical Engineering
Undergraduate Officer

Syngas Production Using a Catalytic Engine

by

Andrea Arce

Submitted to the Department of Mechanical Engineering
on May 8, 2015 in Partial Fulfillment of the
Requirements for the Degree of

Bachelor of Science in Mechanical Engineering

ABSTRACT

There are many industrial processes, such as shale hydraulic fracturing, where small throughput of natural gas is considered a low-value waste or, at best, a nuisance. The natural gas is remote from potential users or from pipelines, making it too expensive to transport to market. As a consequence, it is simply burned (flared) to form carbon dioxide to dampen its environmental impact (i.e. methane has a higher global warming potential than carbon dioxide).

At the Sloan Automotive Laboratory, we have been investigating new processes to convert methane into a valuable liquid fuel product in a compact unit that could avoid the need for flaring, and to do so in an economical way. The processes use internal combustion engines as a chemical reformer to convert natural gas to syngas by means of fuel-rich, incomplete combustion. This thesis project parallels a project that uses homogeneous reforming in-cylinder without a catalyst, with air or oxygen-enriched air (partial oxidation). This experiment explores the use and effects of a catalyst deposited on metallic foams placed in a one-cylinder compression-ignition engine, operating either in partial oxidation mode in combination with dry reforming. The metallic foam is attached to the bowl in the piston to carry out the chemical reaction. We determine composition of the reformate to determine conversion and selectivity. The product composition is determined with a gas chromatography. The metal foam catalyst is an effective means of syngas generation. We explore the impact of changing parameters such as equivalence ratio, CO2 content, and intake temperature and pressure.

Thesis Supervisor: John G. Brisson
Tile: Professor of Mechanical Engineering

ACKNOWLEDGEMENTS

Thank you to my parents, sisters and friends for helping me get through MIT this past 4 years.

Thank you to Emmanuel Lim, Dr. Leslie Bromberg and Dr. John Brisson for allowing me to perform the experiments and giving me advice and guidance through the process.

TABLE OF CONTENTS

LIST OF FIGURES

LIST OF TABLES

CHAPTER 1
INTRODUCTION

In the United States, there is a surplus of natural gas due to the development of horizontal drilling and hydraulic fracturing. Most of this natural gas surplus is driven by the development of the shale industry. The oversupply of natural gas has resulted in very low gas prices in the US, making use of stranded gas challenging. As a consequence, the gas industry has great interest in developing technologies that allow converting this gas into something profitable.

Many economic factors affect whether stranded gas should be extracted from the ground, left as is, burned as a waste product or converted into liquid fuel. When transportation of this gas is of high cost, the natural gas is abandoned or flared into the atmosphere. For example, in North Dakota, over one third of the gas produced, as associated gas (that is, as a byproduct of the production of oil) was flared in 2011. [1] Throughout the United States, wells with flaring produced between 400,000 and 1,500,000 scfd of natural gas in 2009. [2] This is about three to four orders of magnitude smaller amount of gas than those found on large gas-to-liquid plants. However, these large gas-to-liquid plants cannot serve individual or groups of wells because the technology does not scale economically to small size.

There is a strong interest in developing smaller economically competitive gas-to-liquid (GTL) plants. The first stage of a gas-to-liquid plant is the syngas production unit, followed by a syngas conditioner and a liquid fuel synthesis reactor. Methanol is an attractive liquid since it is easier to transport to the market. The best way to reduce the cost of the plant is by

reducing the cost of the syngas production unit, which accounts for roughly 60% of the total plant cost with the remaining 40% goes into liquid fuel synthesis. Using an engine as a chemical reactor could potentially reduce the capital cost of the plant.

In the Sloan Automotive Laboratory at MIT, we are exploring methods for converting methane into syngas, using internal combustion engines. The engines are running as chemical reactors, in an unconventional way to produce syngas. Compression ratio, intake temperatures, gas compositions (including equivalence ratio) and intake pressures are all variables that can be changed to achieve certain methane conversion efficiency. The results of these experiments have shown the conversion of methane to syngas with high methane conversion efficiency and adequate selectivity. The syngas making engines are inexpensive, compact and with relatively high throughput, enabling a compact micro-GTL plant.

This thesis describes an alternative approach where a one-cylinder compression-ignition engine is used as a catalytic chemical reactor to convert methane into syngas. The objective is to improve the selectivity by operating at higher equivalence ratios than possible with a homogeneous engine. A catalyst deposited on metal foam is placed rigidly in the bowl of the piston to carry out the chemical reaction. The foam occupies roughly 40% of the clearance volume, which indicates that roughly 40% of the methane should be converted into syngas (the gas in the foam is colder than the gas in the unoccupied region, increasing the mass of the cylinder charge that is in contact with the catalyst). The composition of the products is measured with an online gas chromatography. The results are used to see the effects of the catalyst in the conversion of this natural gas.

CHAPTER 2
ENGINE REFORMER

2.1 Diesel Engine Operation

The project used a modified diesel engine as the chemical reactor. To understand how a diesel engine is used as a reactor, it is important to know how it works.

Diesel engines are compression-ignition (CI) internal combustion engines. In contrast with spark-ignition (SI) engines, the compression-ignition engine does not rely on an external source, e.g. spark discharge, to initiate combustion in the cylinder. In a compression-ignition engine, the combustion is initiated when the air-fuel mixture is compressed and heated. Diesel engines are not throttled, so the load in the combustion chamber is controlled by the amount of fuel injected. Modern diesel engines make use of direct-injection (DI), where the fuel injector sprays the fuel directly inside the cylinder at high pressure. In these modern direct-injection diesel engines, only air is inducted into the cylinder. A physical schematic of a diesel engine is shown in Figure 2.1.

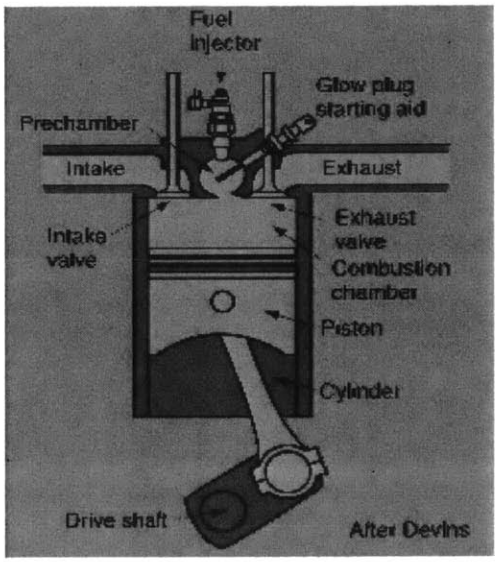

Figure 2.1: A schematic of a diesel engine [3]

This intake air is compressed during the compression stroke to around 30 to 55 bar in naturally aspirated (NA) engines, or 80 to 110 bar in supercharged engines, reaching temperatures of 700 to 900 °C. Before the piston reaches Top Dead Center (TDC) or highest position, the fuel is rapidly injected into the cylinder. Because of the extremely high fuel injection pressures (1000 to 2000 bar in modern engines), the liquid fuel jet is atomized and can then entrain the already hot, compressed air. High temperatures and pressures in the cylinder permit the evaporation of the liquid fuel, which mixes with the air. Once the temperature and pressure are above the fuel's ignition point, the non-uniform fuel-air mixture spontaneously ignites (autoignition, following a short ignition delay). As energy is released through the heterogeneous combustion process, the pressure increases even more. The burned gas is then expanded and work can be extracted from the engine. Figure 2.2 shows a sample cylinder pressure vs. engine crank angle diagram for a compression-ignition engine.

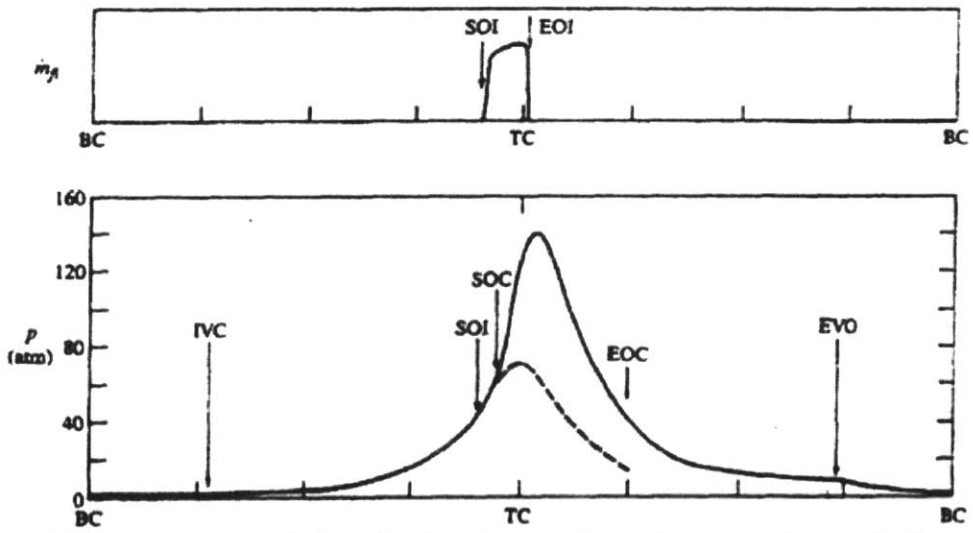

Figure 2.2: Sequence of events during a diesel engine operating cycle: compression, combustion and expansion. The first graph shows fuel injection mass flow rate into the cylinder vs. crank angle. The second graph shows cylinder pressure vs. crank angle. Compression occurs from Bottom Dead Center (BC) to Top Dead Center (TD) having the intake valve closing (IVC) towards the beginning of the compression, and the start of injection (SOI) towards the end. The start of combustion (SOC) occurs right before TC and the end of combustion (EOC) occurs during the expansion. The exhaust valve opening (EVO) happens before the reaching BC. [4, p.28]

The diesel engine is well known for its higher efficiency relative to the conventional gasoline-fueled spark-ignition engine. This higher efficiency is the result of several essential features present in the Diesel engine cycle.The compression ratio, which is defined as the ratio of the total volume to the clearance volume (minimum volume in the combustion chamber when piston is at top center), is much higher than typical SI engine values. In gasoline spark-ignition engines, where the fuel-air mixture is premixed, autoignition is not desired because of the resulting "knock" phenomenon. In SI engines, knock can be damaging. The direct injection in Diesel engines eliminates this knock problem, and allows compression ratios to values of 12 to 24, with 15 being the norm. A second important criteria, which affects the efficiency of Diesel engines is the overall lean operation. Diesel engines must operate lean due to the non-uniformity of the air-fuel mixture, where enough air is necessary to achieve local stoichiometric combustion in the flame. Figure 2.3 shows the fuel conversion efficiency dependence on compression ratio and fuel/air equivalence ratio according to Fuel-Air Cycle results. These cycle simulations deal with accurate properties for the working fluids, but employ ideal cycle calculations. The values for spark ignition engines are in the range of 85% of the ones determined from these Fuel-Air Cycle results.

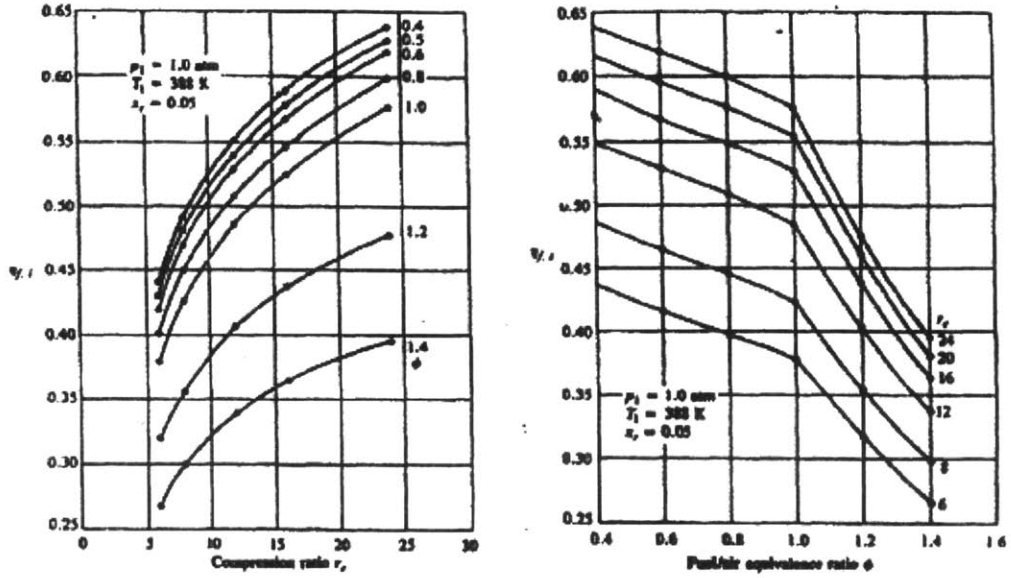

Figure 2.3: Fuel-air cycle results for indicated fuel conversion efficiency as a function of compression ratio and equivalence ratio [4, p.182]

In addition to this higher efficiency due to the overall lean operation, diesels have reduced pumping losses because the air is not throttled. The engine load in diesel engines is controlled by the amount of fuel that is injected into the combustion chamber. This means that the pressure losses at part-load in diesels are much lower than in throttled spark-ignition engines, where the pressure is reduced below atmospheric to control the output of the engine. The thermodynamics of the engine's operating cycle are discussed in more detailed in the following section.

2.2 Thermodynamics of Diesel Engine Operating Cycle

An internal combustion engine operating cycle can be broken down into different processes: intake, compression, combustion, expansion and exhaust. With ideal models for each of the process, the engine's working conditions and efficiency can be approximated. For this thesis, a model was developed that used the simplest models for each of the process,

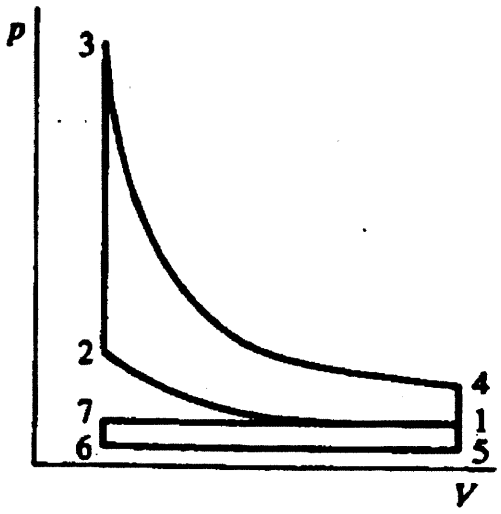

Figure 2.4: Pressure Volume diagram during a diesel engine operating cycle: Compression (1-2), Constant-volume combustion (2-3), Expansion (3-4), Exhaust (4-5-6) and intake (6-7-1). Maximum volume is Bottom Dead Center (BDC) and minimum volume is Top Dead Center (TDC) [4, p.163]

which are explained in detailed in this chapter. Figure 2.4 shows a volume vs. pressure diagram of the engine operating cycle used for this project.

During the intake process (state 6-7-1 in Fig. 2.4), the cylinder volume increases as the pressure differences slightly across open valves. The intake process begins at bottom dead center (BDC) and the pressure is most of the times atmospheric pressure (P_{int} = 1.0 bar). As it is shown in the previous section, the intake valve remains open until the beginning of the compression stroke; however, this is ignored since it is a simple model approximation.

The compression process (state 1-2 in Fig. 2.4) is assumed to be adiabatic and reversible and hence isentropic (i.e., no change in entropy, $S_1 = S_2$). The ratio between the volume at the beginning of the compression process, V_1, and the volume at the end of the compression process, V_2, is equal to the compression ratio (r_c). The compression work (W_c) is equal to the change in internal energy.

For the combustion process (state 2-3 in Fig. 2.4), it is assumed to be a constant-volume process (that is, it is assumed that the process takes place nearly instantaneously at top dead center, TDC). The volume at the beginning of combustion, V_2, is equal to the volume at the end of combustion, V_3.

For the expansion process (state 3-4 in Fig. 2.4), it is assumed to be an adiabatic and reversible process hence isentropic just like the compression process. The enthalpy remains constant ($S_3 = S_4$). The ratio between the volume at the beginning of the exhaust process, V_3, and the volume at the end of the exhaust process, V_4, is equal to the inverse of the compression ratio (r_c^{-1}).

The exhaust process (state 4-5-6 in Fig. 2.4) is similar to the intake process, but in this case, the exhaust valve opens to release the mixture inside the cylinder. The exhaust valve opens before reaching Bottom Dead Center (BDC) and therefore, the exhaust pressure is higher than the intake pressure. Usually, the exhaust pressure is about 1.3 times bigger than the intake pressure. Once, the cylinder reaches BDC then the exhaust pressure does become atmospheric pressure.

2.3 Catalyst and Metal Foam

A catalyst is a substance that increases the rate of a chemical reaction without itself undergoing any permanent changes. With a catalyst, a reaction occurs faster at lower temperatures. Metal foam is a cellular structure that has solid metal, usually copper or aluminum, as well as a large volume fraction of gas-filled pores. When the pores are not sealed, the metal foam is open cell metal foam. Metal foams are used in applications such as heat exchangers, energy absorption and flow diffusion. A combination of these two materials

results in a fast heat transfer rate, which is desired in the production of syngas.

In this project, an iron-chromium-aluminum alloy (FeCrAl) metal foam was coated with a palladium catalyst by Prof. R. Farrauto and his Columbia University team. This material forms a thin layer of alumina on its surface when exposed to air. The alumina substrate binds well to the alumina coating forming a robust assembly that is resistant to erosion. The catalyst helps carry out the chemical reactions while the metal foam helps the gas maintain a near constant temperature. However, the catalyst must be at or above the light-off temperature to carry out the reaction within the time that the gas remains inside the foam, which is near TDC for about 10 milliseconds. This specific foam must be kept at a temperature under 850 °C to avoid sintering the alumina substrate, and closing the pores where the palladium catalyst is deposited. Figure 2.5 shows the metal foam coated with the catalyst.

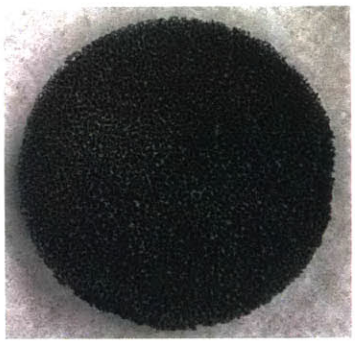

Figure 2.5: Metal foam coated with the catalyst.

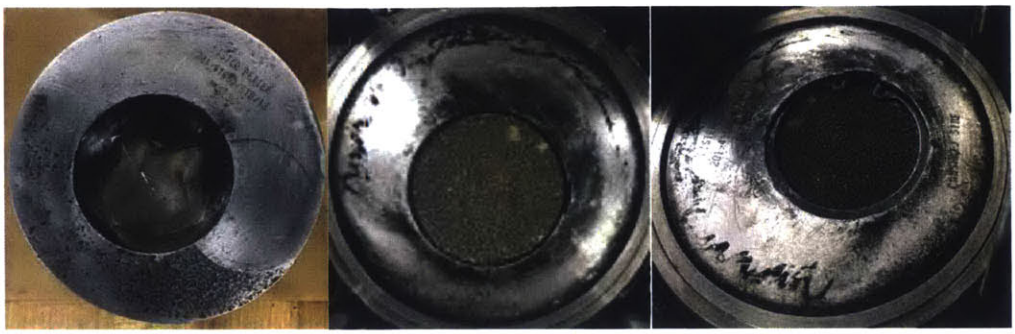

Figure 2.6: Piston head bowl with no foam, with foam, and foam with retaining ring in place.

During the engine tests, the coated metal foam remained inside the piston bowl. To hold the catalyst in place, a groove with a width of 2.16 mm and a diameter of 54 mm was machined around the inner top wall of the piston bowl using a T-Slot cutter on a HASS VF 2 mill. The groove was used to hold in place a steel-retaining ring of a width of 2.01 mm and a diameter of 55.19 mm. Figure 2.6 shows the piston bowl with no metal foam followed by piston bowl with catalyst inside and finally the piston bowl with metal foam and retaining ring in place.

2.4 Chemical Reactions

The main goal of this thesis is to investigate methane conversion to syngas, which is a mixture of CO and H_2. This can be achieved by doing partial-oxidation. Partial oxidation is an exothermic process (-ΔH). The chemical reaction for partial oxidation is shown in Eq. 1.

$$CH_4 + \tfrac{1}{2}O_2 \leftrightarrow CO + 2H_2 \qquad \Delta H^\circ_{298,POX} = -38\ kJ/mol \tag{1}$$

To reduce the amount of heat produced during the reaction, an endothermic process (ΔH) was included: dry reforming uses methane and carbon dioxide as reactants to produce hydrogen and carbon monoxide in a 1:1 ratio. The chemical reaction equation is shown in Eq.

2.

$$CH_4 + CO_2 \leftrightarrow 2H_2 + 2CO \qquad \Delta H°_{298,DR} = 247\ kJ/mol \tag{2}$$

When there are extra moles of CO_2 as reactants, the CO_2 could participate in reverse water gas shift, where the hydrogen produced in the reaction (1) is used up producing water and CO. The reverse water gas shift reaction below is shown in Eq. 3.

$$H_2 + CO_2 \leftrightarrow CO + H_2O \qquad \Delta H°_{298,WGS} = -41\ kJ/mol \tag{3}$$

In addition, the CO_2 is a diluent (with high value of heat capacity) that can be used to moderate the temperature excursion from reaction (1).

The desired process is autothermal reforming (ATR) which utilizes O_2 and H_2O with CH_4. ATR is just a combination of partial oxidation and steam reforming. For this project, only the dry reforming was attempted while the partial oxidation was kept constant because of the issues having to do with the required steam injection associated with steam reforming.

CHAPTER 3
EXPERIMENTAL SETUP

3.1 Engine Setup

The engine chosen for this thesis needed to meet several characteristics. The engine must have good technical support and design information available to be able to make modifications quickly. As explained in an earlier chapter, the goal of using an engine as a chemical reformer was to reduce size and cost, so the engine must be small and not too expensive. Relatively simple disassembly of the engine was also a major concern. The metal foam may have to be replaced frequently, so having an easy to remove head was a very important criterion. A generator set was preferred because a dynamometer is already fitted along with the associated electronics. For the intake and exhaust components, the engine had to be modified, most importantly, disconnecting the fuel system.

The engine chosen for the project was a Lister-Petter TR1 Diesel Generator. It is a single cylinder, naturally aspirated flywheel fan air-cooled diesel engine with a cylinder volume of 0.773 L. The engine was electrically driven with a mechanical governor to operate the engine at steady conditions at desired speed, through the use of a variable speed drive. This related output frequency to revolutions per minute (RPM). The compression ratio is 15.5:1, which is typical for diesel engines. Oil sump capacity is 2.7 liters. The fuel tank in the engine was replaced with the 2 US gallon container as the fuel filter was attached to the cylinder block head, but it was not used during these experiments. Figure 3.1 shows typical features that are seen in the TR/TS 1 engine series except the fuel tank that was replaced.

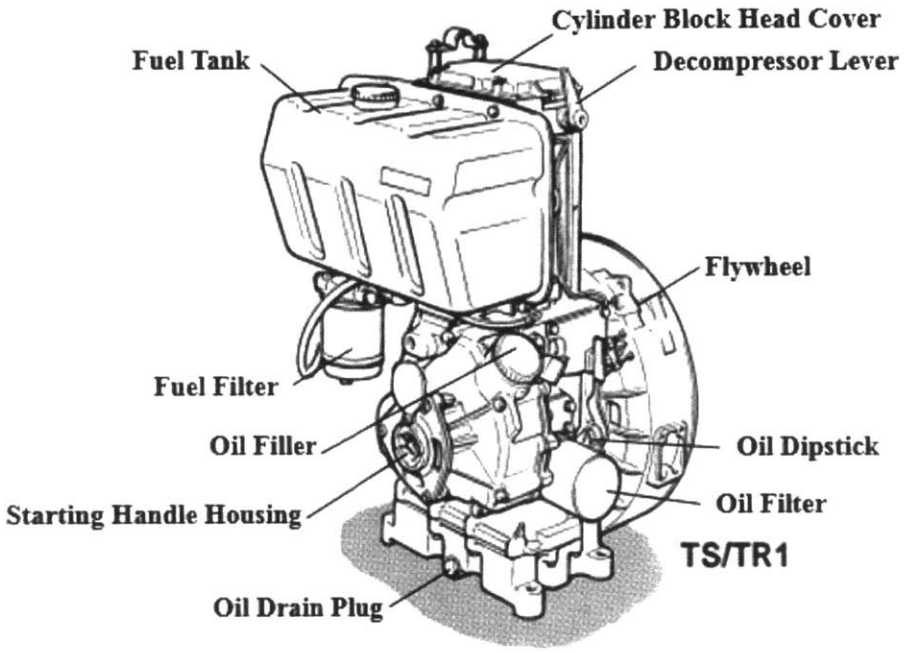

Figure 3.1: Lister-Petter TR/TS1 series engine [5]

Several things were modified to be able to run the desired experiments. The intake and exhaust manifolds had to be welded into the plate. The gaskets in the cylinder head, engine block and head cover had to be replaced with new ones as they were worn out or broken. The oil had to be changed as well as the oil filter. In order to prevent contamination/deactivation of the catalyst by the oil additives, we used a base oil without any additives. These additives incorporate sulfur and heavy metals that could poison the catalyst.

For draining the oil, a clean container was placed under the drain plug that is located in the bottom side of the engine. This made it harder to drain the oil, as it was not on the bottom of the oil sump. Once the used oil was completely drain, new engine oil with no additives was added to the oil sump. The dipstick was checked to ensure the oil was clean and filled to the

top mark. To change the oil filter, a suitable strap wrench was used to unscrew and remove the old oil filter. The crankcase filter housing face was cleaned and a small amount of clean engine oil was applied to the sealing joint. A Wix 51374 Spin-of oil filter was used for this engine. The new oil filter was screwed in and tightened half a turn with the strap wrench. The dipstick was checked again to ensure there was no loss of engine oil. Finally, the engine was run for a few seconds to allow for the new oil to settle in.

The intake temperatures for the air and fuel mixture were adjusted by a set of Omega AHPF-122 1200W air process heaters and one AHPF-082 600W air process heater. Preheating was done to achieve adequate temperature in the catalyst. The gases were provided by 300 L cylinder bottles that were each connected to Omega FMA-2 mass flow controllers. A solenoid valve was placed before each mass flow controller to be able to control the flow from electronically. There was one bottle and one mass flow controller for each gas. After the mass flow controllers, the gases went to the intake manifold. The gases were heated using electrical heaters before going into the cylinder. To minimize heat losses, mineral wool insulation was applied around the heaters. The intake for the oxidizer and fuel were monitored with two thermocouples each located in each heater, and two more thermocouples to measure the intake and exhaust temperature separately close to the valves. Data Instruments Model SA 0-25 PSIA 0-5 Vdc pressure transducers were placed at the intake and exhaust manifold to monitor the pressure of the engine. Figure 3.2 shows the physical modified intake system for this project and Fig. 3.3 shows a schematic of the intake system.

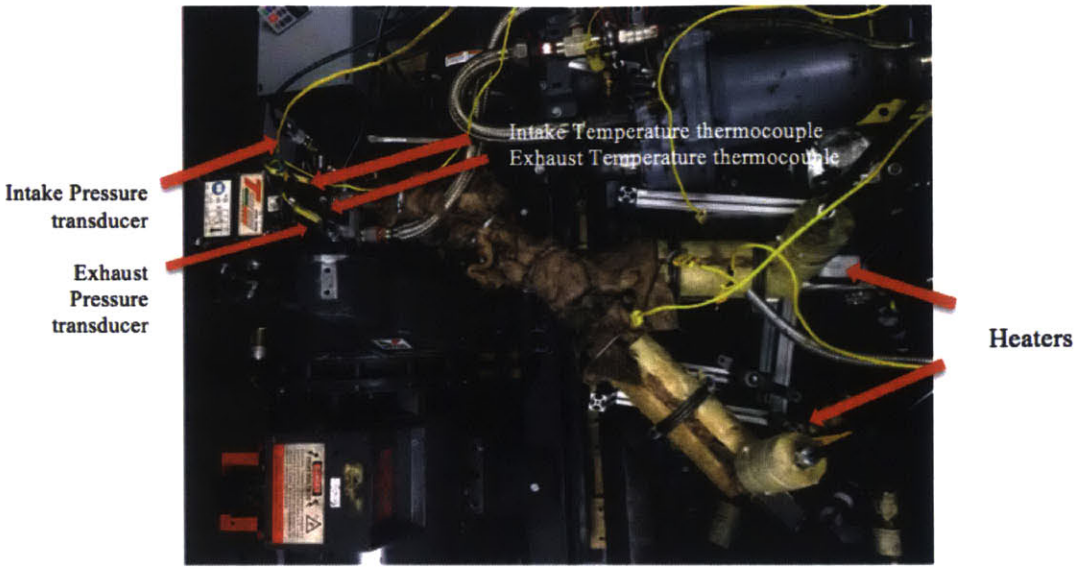

Figure 3.2: Physical intake system showing heaters, thermocouples and pressure transducers.

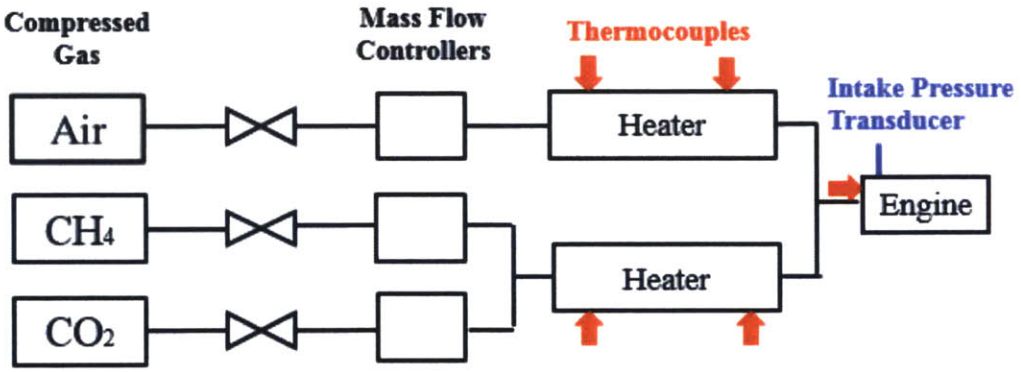

Figure 3.3: Schematic of intake system.

The exhaust gases containing CO and H_2 went in two different directions. Some of the mixture went through a Fives North American "Aardvark" high velocity burner to be combusted to complete oxidation. This step was necessary to be able to comply with the safety regulations of CO release. The remaining exhaust mixture went through the sampling system. This exhaust mixture passed through a counter-flow heat exchanger with cold water to decrease its temperature and to remove water vapor from the mixture, then through a filter

to remove any soot, a desiccant to remove water from the mixture and finally introduced into an Agilent 490 Micro Gas Chromatography (GC). This procedure is done to prevent soot and water from plugging the GC. Figure 3.4 shows part of the physical exhaust sampling system and Fig. 3.5 shows a schematic of the sampling system.

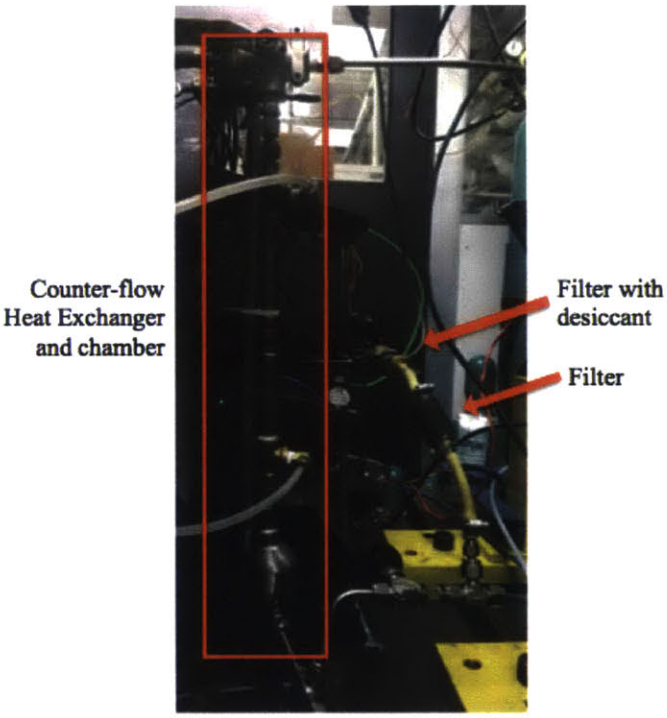

Figure 3.4: Part of sampling system

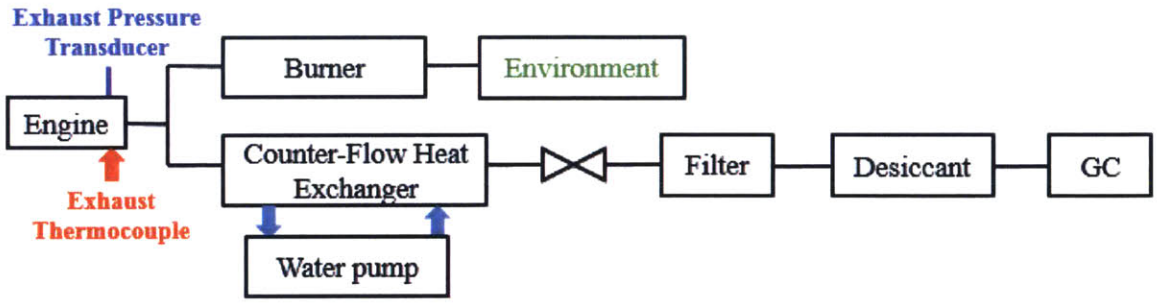

Figure 3.5: Schematic of entire sampling system

3. 2 Mass Flow Rate

To calculate the correct volumetric flow rate that should be given to each mass flow controller, a series of calculations are done depending on the conditions tested. The input gases are CH_4, H_2, CO_2, O_2 and N_2. The chemical reaction equation is shown in Eq. 4.

$$CH_4 + \frac{2}{\phi}(O_2 + 3.773N_2) + Y_{DR}\frac{\Delta H°_{298,POX}}{\Delta H°_{298,DR}}[(CH_4 + CO_2) + (n_{CO2} - 1)CO_2] \quad (4)$$

Φ is the fuel-air equivalence ratio, Y_{DR} is a constant that defines how much dry reforming participates in the reaction with respect to partial oxidation, n_{CO2} is the excess number of moles in the reaction. Some of the variables remain constant while other change throughout data acquisition. Table 1 shows the variables.

Table 1: Engine constant and variant variables

Variable	Value
Φ	4
Intake Temperature (°C)	160-170
Engine Speed (RPM)	750
$\frac{\Delta H°_{298,POX}}{\Delta H°_{298,DR}}$	0.154
Intake Pressure (bar)	1.1
Y_{DR}	0.25, 0.5,0.75, 1
n_{CO2}	1, 2, 3, 4, 5

The total number of moles, n_{total}, needs to be calculated to find the mole fraction of each of the gases. Equation 5 shows the total number of moles in the reaction and using Eq. 6, the mole fraction, $\bar{x}_i$, of each component was calculated.

$$n_{total} = 1 + \frac{2}{\phi}(1 + 3.773) + Y_{DR}\frac{\Delta H°_{298,POX}}{\Delta H°_{298,DR}}[1 + n_{CO2}] \quad (5)$$

$$\overline{x_i} = \frac{n_i}{n_{total}} \quad (6)$$

Once the mole fraction is known, the mass of the mixture, M_i, is calculated by adding all of the masses of the gases. Mass equation used for each of the components is shown in Eq. 7.

$$M_i = \sum(\overline{x_i} \times MW_i) \quad (7)$$

Then, the mass fraction, x_i , of the gases is calculated with Eq. 8.

$$x_i = \frac{M_i}{M_{mix}} \quad (8)$$

The total mass flow rate that goes into the engine, $\dot{m}_{engine}$, is calculated by using the total mass going into the engine, M_{mix} , the intake pressure, P_i , intake temperature, T_i , engine speed, N, and displacement volume, V_d, as shown is Eq. 9.

$$\dot{m}_{engine} = \frac{N \times V_d \times P_i \times M_{mix}}{2 \times R \times T_i} \quad (9)$$

Mass flow rate for each of the gases is calculated by using equation 10.

$$\dot{m}_i = x_i \times \dot{m}_{engine} \quad (10)$$

The density registered for each gas in each of the mass flow controllers is known. Equation 11 is used to find the volumetric flow rate of each of the gases.

$$\dot{V}_i = \frac{\dot{m}_i}{\rho_i} \quad (11)$$

With the calculations above, each mass flow controller gets a correct flow rate.

3.3 Data Collection and Processing

As stated in chapter 3.1, a sample line was drawn from the main engine exhaust and

cooled by a counter flow heat exchanger with cold water to remove water vapor, then through a filter and desiccant. The cooled and dried gas was drawn with a KNF Neuberger UN726FTP diaphragm vacuum pump through a Parker 9900-05-BK Balston filter and Drierite 10-20 mesh anhydrous indicating desiccant to remove particulate matter and water vapor. This gas was then analyzed in an Agilent 490 Micro GC using settings described in Table 2. Two columns were used in the GC with a thermal conductivity detector. MS5A was used to detect H_2, O_2, N_2, CH_4, and CO. PPU was used to detect CO_2. Each column was operated under different conditions to be able to detect the gas.

Table 2: Information about Agilent 490 Micro GC sampling system.

	CP-Molsieve 5A (MS5A)	**PoraPLOT U (PPU)**
Carrier Gas	Argon	Helium
Injector Temperature (°C)	110	
Injection Time (ms)	40	
Backflush Time (s)	11	N/A
Column Temperature (°C)	80	50
Initial Pressure (kPa)	150	
Sampling Frequency (Hz)	100	
Run Time (s)	150	
Stabilizing Time (s)	5	
Sample Time (s)	90	
Sample Line Temperature (°C)	37	

Once the GC data was collected, the data processed using Agilent OpenLAB software and MATLAB.

To be able to process the data with accurate values, the GC needed to be calibrated before each engine run. The composition of the calibration gases in shown in Table 3.

Table 3: Composition of gases used to calibrate GC

Gas	Composition
1	20% CO_2
2	80% N_2
3	40% H_2
4	21% O_2
5	20% CH_4
6	10% CO

CHAPTER 4

RESULTS AND DISCUSSION

4.1 Catalyst Information and Light-off Temperature

The experimental data was collected throughout three different engine runs. The calibration taken during each of the engine runs was done with the same calibration gases and we found the calibration to be reproducible and stable. A total of three identical catalysts foams were used to take the entire data samples. They were weighed before placed in the piston to make sure the masses agreed with the provided information. The ratio of volume of the catalyst, V_{cat}, to clearance volume, $V_c = 0.5$ L, was around 0.4 for the three samples. Table 4 has information about each of the catalysts samples used.

Table 4: Information about Catalyst

Catalyst Number	Uncoated Weight (g)	Final Weight (g)	Wt of washcoat (g)	Bulk Volume of Catalyst (cm^3)	V_{cat}:V_c
1	8.7114	9.0521	0.3407	20.21	.404
2	8.432	8.8485	0.4165	19.95	.399
3	8.4249	8.6531	0.2282	19.92	.398

All of the data samples were taken at a temperature of 160-170 °C. The other variables used during testing can be found in table 1. To be able to take samples, the catalyst needed to be at the light-off temperature. The catalyst had a light-off when the temperature of the inlet was 145 °C for all catalysts. After catalyst light-off, the exhaust temperature would rise at a rate of 1°C per second while the intake temperature would rise at a rate of 0.2 °C per second. Temperature data was recorded for each of the engine runs every 15 seconds and averaged

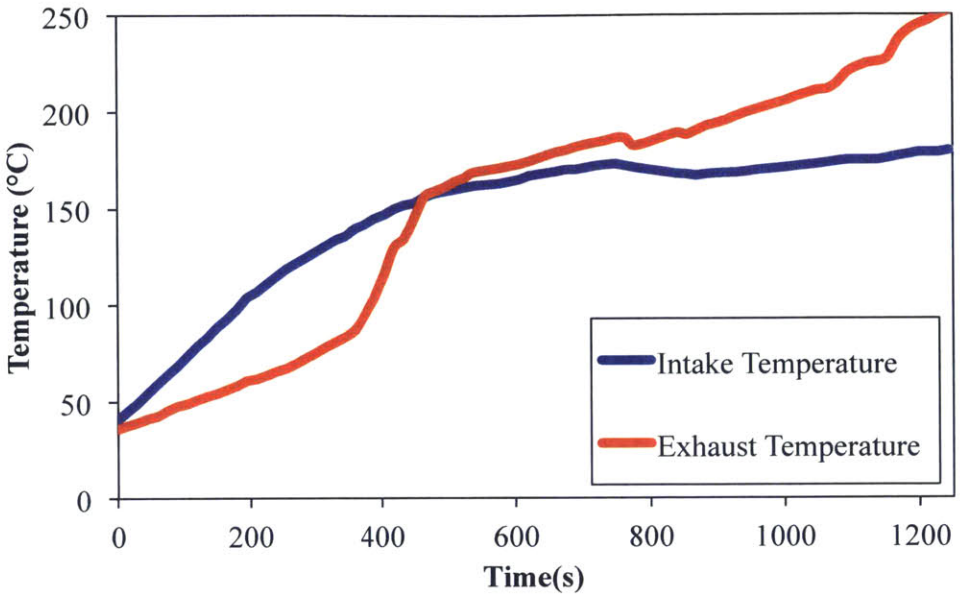

Figure 4.1: Intake and Exhaust Temperature as a function of time during light-off. The largest increase in temperature can be seen between 365 and 450 seconds.

out. The intake and exhaust temperature were plotted versus time. Figure 4.1 shows this data during light-off.

The rapid increase in exhaust temperature at 365 and 450 seconds indicates catalyst light-off, with a rapid temperature increase from 75 to 160 °C. As mentioned earlier in the chapter, all of the data was taken with an inlet temperature of around 160-170 °C, once the exhaust temperature "stabilized" again or had a lower temperature rate of change.

4.2 Conversion Efficiencies and Carbon Balance

Conversion efficiencies of CH_4 and CO_2 were calculated by normalizing the flows of methane and CO_2 to the flow rate of nitrogen (as described above). There are very little, if any NO generation in the process, due to the rich nature of the combustion; indeed, the GC did not detected any NO_x gases. The conversion efficiency of CO_2 was recorded to understand how much of the CO_2 was actually reacting during the chemical reaction. As mentioned in previous chapters, the CO_2 gas was used to control the catalyst temperature to protect the

catalyst from reaching very high temperatures and potentially, burning. To calculate the conversion efficiencies of CH_4 and CO_2, the moles in the intake had to be compared to the moles in the exhaust with respect to the moles of N_2 in the intake and exhaust. The conversion efficiency of CH_4 is expressed as X_{CH_4} in Eq. 12 and the conversion efficiency of CO_2 is expressed as X_{CO_2} in Eq. 13. While the conversion of CH_4 is straight forward, the conversion of CO_2 is much more complex because the partial oxidation of methane could generate some CO_2, and CO_2 could participate in water-gas shift reaction with the hydrogen produced. The intake mole fractions for each of the components are determined from the intake composition using Eqs. 5, 6 and 7 expressed in chapter 3.2.

$$X_{CH_4} = \frac{x_{CH_4,exh}}{x_{CH_4,int}} \times \frac{x_{N_2,int}}{x_{N_2,exh}} \times 100\% \tag{12}$$

$$X_{CO_2} = \frac{x_{CO_2,exh}}{x_{CO_2,int}} \times \frac{x_{N_2,int}}{x_{N_2,exh}} \times 100\% \tag{13}$$

The conversion of efficiency of CH_4 for all of the data samples is shown in Fig. 4.2.

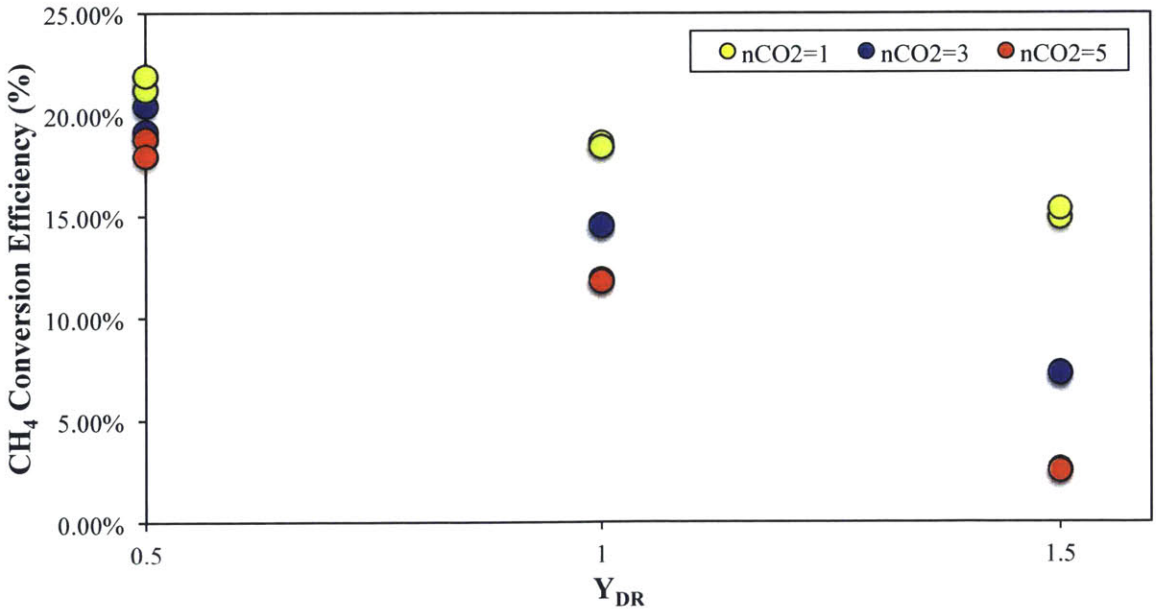

Figure 4.2: Conversion Efficiency for CH_4 for intake temperature between 160 and 170 °C with different intake number of moles of CO_2.

The conversion efficiency of CH_4 showed to be best at smallest ratio of exothermic to endothermic reaction between partial oxidation and dry reforming ($Y_{DR} = 0.5$) and with no excess CO_2 in the intake ($n_{CO2} = 1$). Even at a higher Y_{DR} (1 and 1.5), the conversion still proved to be highest with no excess CO_2 in the intake. This can be due to the fact that the gas temperature in the foam is higher (the case as a higher value of gamma with reduced CO_2 diluent) allowing for the catalyst to perform and react better with the reagents. Also, as calculated in section 4.1, the ratio of catalyst volume to clearance volume is for the three samples around 0.3. Assuming the catalyst is reacting at Top Dead Center (TDC), only around 20% of the methane is converted into syngas because catalyst volume is 30% of clearance volume. In an ideal case, the 30% of the methane should be converted into syngas because of the ratio between catalyst and clearance volume.

The conversion efficiency of CO_2 for all of the data samples taken is shown in Fig. 4.3.

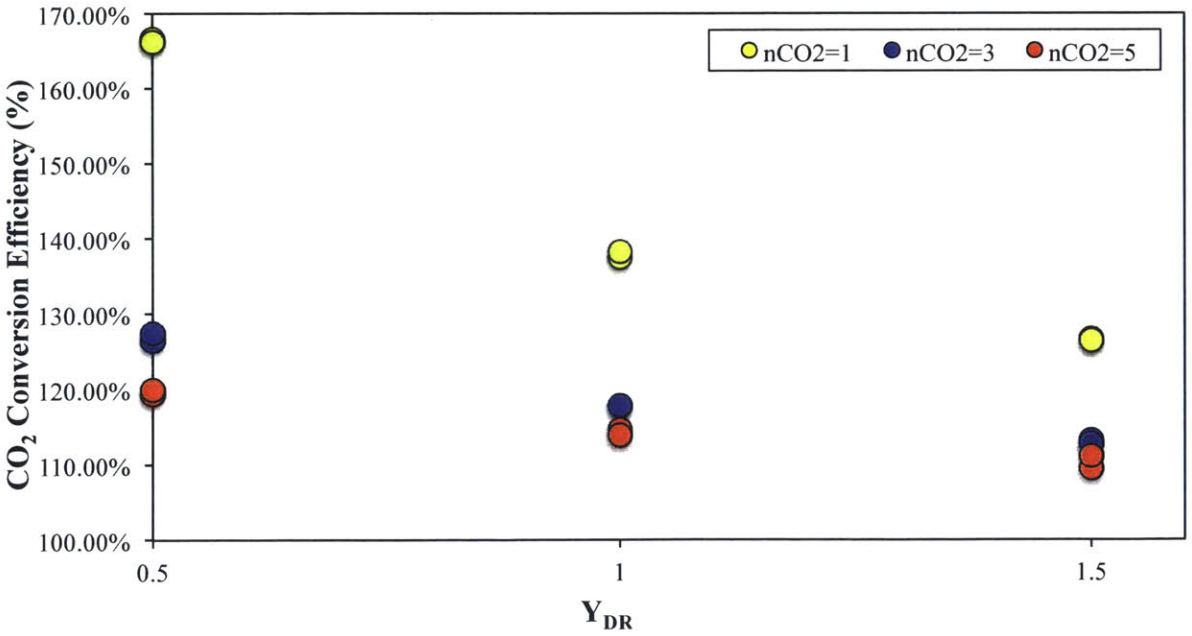

Figure 4.3: Conversion Efficiency for CO_2 for intake temperature between 160 and 170 °C with different intake number of moles of CO_2.

The conversion efficiency of CO_2 is best when Y_{DR} equals 0.5 and the $n_{CO2} = 1$. The results in Figure 4.3 indicate that CO_2 flows did not change much through the process. It is possible that some of the CO_2 in the reagents reacts with the hydrogen (generating water and CO, in the reverse water-gas-shift reaction), thus increasing both water and CO concentration, with decreased hydrogen concentration. For most of the data samples, the ratio between the CO_2 flow rates in the outlet to that in the intake remained between 100% and 125% (that is, there is more CO_2 flow rate in the exhaust than in the inlet, increasing the amount of CO_2). However, as Y_{DR} increases, the best conversion efficiency is seen with the higher number of moles of CO_2 in the intake. Given that the intake amount of CO_2 is greater at five than at one, there is more accuracy at the five moles of CO_2 allowing for a smaller error. At five, there is so much extra CO_2 that the conversion efficiency is more precise.

The results have been used to obtain a mass balance for carbon. Mass balances of hydrogen and oxygen are difficult because we are not monitoring water. The molar flow rate of carbon coming into the engine should be equal to the molar flow rate of carbon coming out of the engine, unless there is large amounts of soot (solid carbon) being made. The carbon balance equation is shown in Eq. 15.

$$C_{Balance} = \frac{x_{CH_4,exh} + x_{CO_2,exh} + x_{CO,exh}}{x_{CH_4,int} + x_{CO_2,int} + x_{CO,int}} \times \frac{x_{N_2,int}}{x_{N_2,exh}} \quad (15)$$

The carbon balance for the data samples taken in the three engine runs is shown in Fig. 4.4.

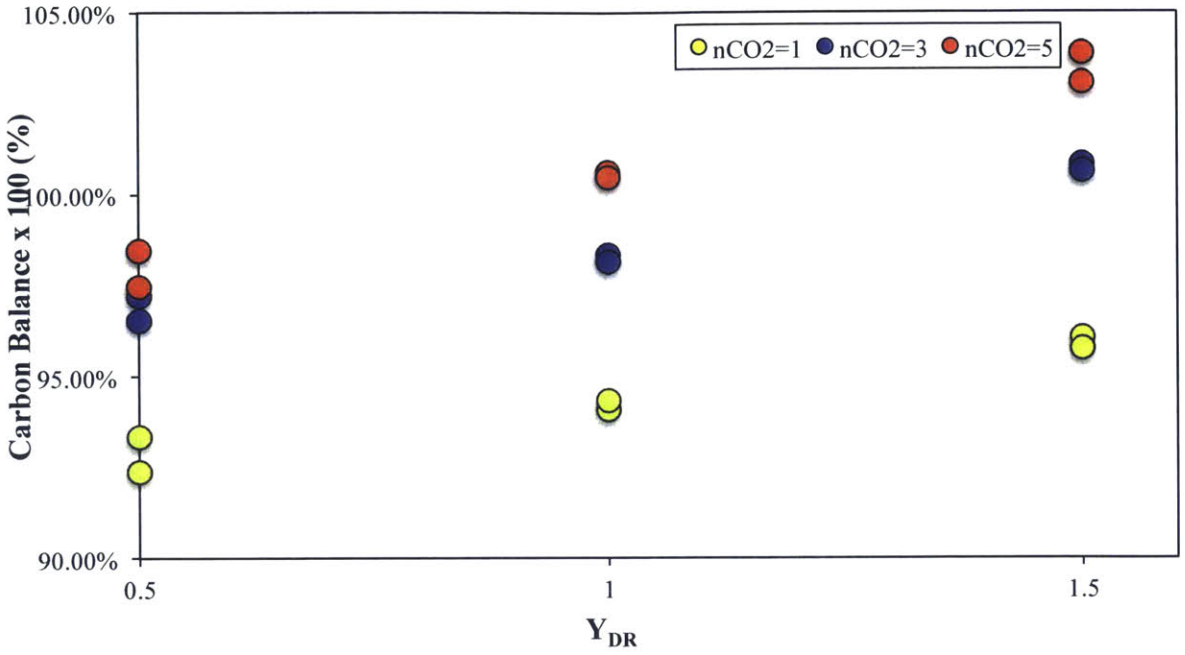

Figure 4.4: Carbon Balance for all data samples.

For the majority of the data samples, the carbon balance stay within ±12.5%. However, the data points closer to the 100% carbon balance, which means the same number of carbon atoms coming in and out of engine, correspond to those with the number of moles of CO_2 equal to 3. The ones with the least amount of carbon in the exhaust are the data points with the number of moles of CO_2 equal to 1. One possibility for having less carbon in the exhaust than in the intake is that solid carbon was made in the cylinder in the form of soot. The least amount of soot is made with the number of moles of CO_2 equal to 3 and 5.

Important information to measure from the exhaust mixture is the moles of H_2 and moles of CO. The desirable ratio of moles of H_2 to moles of CO should be close to 2.0 as this is the requirement for liquids synthesis downstream from the syngas generator reactor. Figure 4.5 shows the ratio between the two gases for all of the data samples.

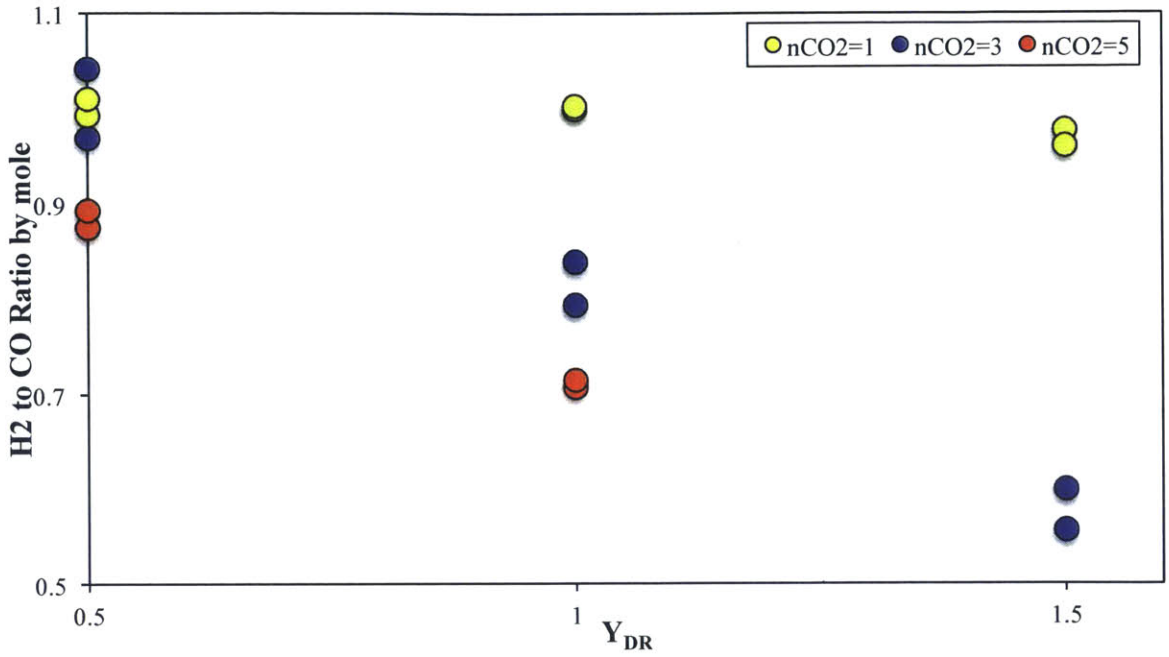

Figure 4.5: Hydrogen to Carbon Monoxide Ratio by mole for all of the samples taken.

The results show that the higher ratios correspond to Y_{DR} equal to 0.5 and number of CO_2 moles equal to 1. Even at different Y_{DR}, the best results are seen with no excess CO_2 at the intake ($n_{CO2} = 1$). As Y_{DR} increases (leaning more towards dry-reforming) the H_2 to CO ratio decreases, and also decreases with a fix Y_{DR} as the number of CO_2 moles increase (n_{CO2} increases). As observed in the conversion of CH_4, the best and highest conversions were found with the least number of CO_2 moles and the highest conversion was found at Y_{DR} equal to 0.5 and one mole of CO_2.

These results show that the best conditions to run this catalytic engine is with Y_{DR} equal to 0.5 and the least amount of moles of CO_2 ($n_{CO2} = 1$). The catalytic engine provides more desirable results for liquids synthesis under these conditions such as conversion and H_2/CO ratio. In future work, the effects of increasing catalyst volume could be studied to understand if it provides better results for the production of syngas.

CHAPTER 5
CONCLUSION

In this thesis, the effects of placing metal foam coated with a catalyst inside the piston bowl of a one-cylinder compression-ignition engine during syngas production were investigated. The goal of the project was to understand and experiment with the catalyst to see the impact in syngas production. There were three identical catalysts used throughout the entire engine testing. By measuring the composition of the exhaust mixture with a 490 Agilent Micro GC, important and desired information was calculated. The important measurements to know were the conversion efficiency for CH_4 and CO_2, the H_2 to CO ratio and the carbon balance.

After three engine-testing procedures, the sampling data showed promising results by using the catalyst-in-cylinder. The maximum conversion efficiency for CH_4 showed to be about 20% and the best H_2 to CO ratio showed to be around 1.1. It can be concluded from these results that the catalyst it is working properly because the catalyst volume makes up for 40% of the clearance volume. The best results were obtained with the smallest number of moles of CO_2, ($n_{CO2} = 1$), and the smallest Y_{DR}, which is 0.5. The data proved that the catalyst favors ideal partial oxidation ($\phi = 4$) over dry reforming. Although, dry reforming seemed to still be required for the catalyst because of the need of CO_2 to reduce in-cylinder temperature. As seen in the results, most of the CO_2 does not react during the chemical reaction. However, the conversion efficiency of CO_2 opened the question of whether another non-reactive gas such as N_2 or water can be used instead of CO_2 and act like CO_2 did during the reaction.

In future work, there are many areas to explore from this project. Some of these topics to explore are the effects of a larger volume fraction of the foam catalyst in the cylinder, instead of dead clearance volume, using other non-reactive gases in the intake such as N_2 or steam instead of CO_2 to control in-cylinder temperature while allowing the catalyst to perform at its best; using another catalyst composition; understanding light-off temperature for the catalyst and at what temperature does this exactly happen with different intake compositions; measure the limits of the catalyst, in particular, the catalytic lifetime; explore intake temperatures limits on the catalyst. There are many more areas and topics that can be studied for this innovative system. This project was the first stepping-stone to an interesting and promising system.

REFERENCES

1. U.S. Energy Information Administration, "Over one-third of natural gas produced in North Dakota is flared or otherwise not marketed," 23-Nov-2011...
2. U.S. Energy Information Administration, "United States Total Distribution of Wells By Production Rate Bracket," (2010).
3. Rotec Design Ltd. - http://www.rotecdesign.com/OperatingCycle/4stroke.html
4. Heywood, John B. *Internal Combustion Engine Fundamentals.* McGraw-Hill, Massachusetts Institute of Technology, McGraw-Hill, Inc, 1988.
5. Lister-Petter TS and TR Operators Handbook.